

# Localized Accumulation of Tau without Amyloid-Beta in Aged Brains Measured with [11C]PBB3 and [11C]Pib Positron Emission Tomography

Takayuki Kikukawa<sup>1</sup>, Haruna Saito<sup>1</sup>, Itsuki Hasegawa<sup>1</sup>, Jun Takeuchi<sup>1</sup>, Akitoshi Takeda<sup>1</sup>, Joji Kawabe<sup>2</sup>, Yasuhiro Wada<sup>3</sup>, Aya Mawatari<sup>3</sup>, Yasuyoshi Watanabe<sup>3</sup>, Soichiro Kitamura<sup>4</sup>, Hitoshi Shimada<sup>4</sup>, Makoto Higuchi<sup>4</sup>, Tetsuya Suhara<sup>4</sup> and Yoshiaki Itoh<sup>1\*</sup>

<sup>1</sup>Department of Neurology, Osaka City University Graduate School of Medicine, Asahimachi 1-4-3, Abenoku, Osaka, Japan

<sup>2</sup>Department of Nuclear Medicine, Osaka City University Graduate School of Medicine, Asahimachi 1-4-3, Abenoku, Osaka, Japan

<sup>3</sup>RIKEN Center for Life Science Technologies, Kobe, Japan

<sup>4</sup>Department of Functional Brain Imaging Research (DOFI), Clinical Research Cluster, National Institute of Radiological Sciences (NIRS), National Institutes for Quantum and Radiological Science and Technology (QST), Chiba, Japan

## Abstract

**Objective:** Different regional specificity in tau accumulation is well known in Alzheimer's disease (AD) brains. However, little is known about such distribution in aging brains and mild cognitive impairment (MCI) brains.

**Methods:** Cognitive functions and regional accumulation of tau and amyloid  $\beta$  ( $A\beta$ ) were evaluated in 13 healthy controls (HCs), 3 patients with MCI and 4 AD patients. Tau and  $A\beta$  accumulation was semi-quantitatively measured with positron emission tomography (PET) using [11C]pyridinyl-butadienyl-benzothiazole 3 (PBB3) and [11C]Pittsburgh compound-B (PIB).

**Results:** Age-dependent accumulation of tau was found in all predetermined regions characteristic of AD, especially in the parahippocampal gyrus, lateral temporal cortex, frontal cortex, and posterior cingulate gyrus, where age-dependency was statistically significant. In contrast, age-dependency in accumulation of  $A\beta$  was not observed in most regions assessed in HC. Moreover, the accumulation of tau in regions characteristic of AD in MCI patients was higher than that in HC, whereas tau accumulation was highest and statistically significant in AD patients. Unlike HC, the accumulation of tau was accompanied by that of  $A\beta$  in patients with MCI and AD.

**Conclusion:** Mild and age-dependent accumulation of tau without  $A\beta$  was found in AD-related areas in aging brains. Considering age as a major risk for AD, higher accumulation of tau may trigger the neurodegenerative process of AD.

**Keywords:** Aging; Dementia; Alzheimer's disease; Preclinical; Mild cognitive impairment; Biomarker; Parahippocampal gyrus

## Introduction

Neuropathologically aggregated tau is abundantly found in neurofibrillary tangles (NFTs) of Alzheimer's disease (AD) brains [1]. According to the "Braak stages", NFTs are limited to the transentorhinal region (I-II) and spread to limbic (III-IV) and isocortical association areas (V-VI) [2]. In contrast, low levels of tau are also often found in aging brains without amyloid  $\beta$  ( $A\beta$ ) accumulation (primary age-related tauopathy: PART) [3]. The clinical significance of age-dependent tau deposition without  $A\beta$  is controversial. Some studies suggest that it has a triggering effect on the neurodegenerative process of AD [4,5], while others suggest an  $A\beta$ -independent pathophysiological role [6].

Recently, [11C]pyridinyl-butadienyl-benzothiazole 3 (PBB3) has been developed as a specific tracer of tau used in positron emission tomography (PET) [7]. In average cerebral cortices, PBB3 accumulation is reported to be higher in aged healthy controls (HCs) than in younger ones, although the regional specificity and interaction with  $A\beta$ , which may be the key process in the pathogenesis of AD, have not been elucidated [8].

In the present study, we measured the regional accumulation of tau and  $A\beta$  in HCs of various ages and compared the data with those of patients with mild cognitive impairment (MCI) and AD.

## Materials and Methods

### HC

Subjectively healthy volunteers without history of brain disorders were openly recruited as candidates. Detailed medical histories were obtained through interviews conducted by a board-certified

neurologist. Thorough neurological examinations, including general cognitive function tests, were performed by the same neurologist. The mini-mental state examination (MMSE), revised Hasegawa dementia scale (HDS-R) and Rivermead behavioral memory test (RBMT) was scored by qualified clinical psychologists. Blood samples were collected to evaluate general physical conditions. Magnetic resonance images (MRIs) were also evaluated.

Exclusion criteria were as follows: 1) history of any brain diseases, history of brain surgery, head trauma requiring hospitalization; 2) high risks for cerebrovascular diseases, including poorly controlled diabetes, dyslipidemia and high blood pressure; 3) any neurological findings suggesting brain disorders; 4) cognitive test indicating border-zone or worse level; 5) MRI lesions including asymptomatic lacunas, severe white matter lesion, many cerebral microbleeds and atrophy beyond average for their age. Amyloid PET imaging was not employed for the exclusion of enrollment, although the images were taken in all cases. No other biomarkers were examined in the HC group.

**\*Corresponding author:** Yoshiaki Itoh, Department of Neurology, Osaka City University Graduate School of Medicine, Osaka, 545-8585, Japan, Tel: +81-6-6645-3889; Fax: +81-6-6646-5599; E-mail: [y-itoh@med.osaka-cu.ac.jp](mailto:y-itoh@med.osaka-cu.ac.jp)

**Received** October 26, 2017; **Accepted** November 16, 2017; **Published** November 23, 2017

**Citation:** Kikukawa T, Saito H, Hasegawa I, Takeuchi J, Takeda A, et al. (2017) Localized Accumulation of Tau without Amyloid-Beta in Aged Brains Measured with [11C]PBB3 and [11C]Pib Positron Emission Tomography. J Alzheimers Dis Parkinsonism 7: 401. doi: [10.4172/2161-0460.1000401](https://doi.org/10.4172/2161-0460.1000401)

**Copyright:** © 2017 Kikukawa T, et al. This is an open-access article distributed under the terms of the Creative Commons Attribution License, which permits unrestricted use, distribution, and reproduction in any medium, provided the original author and source are credited.

## MCI and AD

Cases with MCI and sporadic AD were recruited from patients attending the outpatient clinic of Osaka City University Hospital. Medical history and neurological findings were evaluated by neurologists specializing in dementia. MMSE, HDS-R, and RBMT were scored by qualified clinical psychologists. MRIs of the brain, including the coronal section, were acquired.

The diagnostic criteria of MCI due to AD by the National Institute on Aging-Alzheimer's Association workgroups were employed for the diagnosis of MCI [9]. Namely, patients with MCI should have cognitive concern reflecting a change in cognition reported by patient or informant. In addition, objective evidence of impairment in memory was assessed with clinical dementia rating (CDR) and CDR score of 0.5 was regarded as MCI. To better understand the role of tau compared to A $\beta$  in the development of AD, MCI was diagnosed regardless of the findings of amyloid or tau PET imaging. For the diagnosis of AD, International Working Group criteria for typical AD (IWG-2) were employed with amyloid PET as in vivo evidence of AD pathology [10]. Cases suggesting familial AD were not included in the present study, though genetic testing was not performed.

Written informed consent was obtained from all participants or from close family when the participants were cognitively impaired. The present study was approved by the Institutional Research Ethics Committee of Osaka City University Graduate School of Medicine (IRB# 1735).

## PET data acquisition

[11C]PBB3 and [11C]Pittsburgh compound-B (PiB) were produced as previously reported [7,11,12]. PBB3 PET images and PiB images were acquired with a Siemens Biograph16 scanner (Siemens/CTI,

Knoxville, TN, USA) and with an Eminence-B PET scanner (Shimadzu Co., Kyoto, Japan), respectively.

For tau imaging, [11C]PBB3 in the range of 370 MBq (Body Weight  $\leq$  50 kg) to 555 MBq (Body Weight  $\geq$  70 kg) was intravenously injected in a dimly lit room to avoid its photoracemization. A 60 min PET scan was performed in the list mode. The acquired data was sorted into dynamic data of 6  $\times$  10 s, 3  $\times$  20 s, 6  $\times$  60 s, 4  $\times$  180 s, 8  $\times$  300 s frames.

For A $\beta$  imaging, each subject received 400 to 500 MBq of [11C] PiB intravenously over 1 min. After the injection, static scan image acquisition was performed for 50 to 70 min.

PET images for PBB3 and PiB were reconstructed by filtered back projection using a 4 mm FWHM Hanning filter and a 5 mm FWHM Gaussian filter with attenuation and scatter correction, respectively.

## Image analysis

Acquired PET images were first corrected for motion artefacts and then pre-processed using PMOD software version 3.7 for PBB3 (PMOD Technologies Ltd., Zürich, Switzerland). Axial and coronal images of T1-weighted MRI were acquired additionally for stereotactic standardization. Accumulation of PBB3 and PiB was measured quantitatively in the regions of interest (ROI), which were set manually on standardized MRI (Figure 1). The standardized uptake value ratio (SUVR) was calculated by dividing area-averaged accumulation of tracers in each ROI by that in the cerebellum at 30 to 50 min after injection of PBB3 and at 50 to 70 min after injection of PiB, respectively. To facilitate visual presentation of SUVR images, PBB3 accumulation outside the brain on MR images in each case, including bone marrow and venous sinuses, was manually

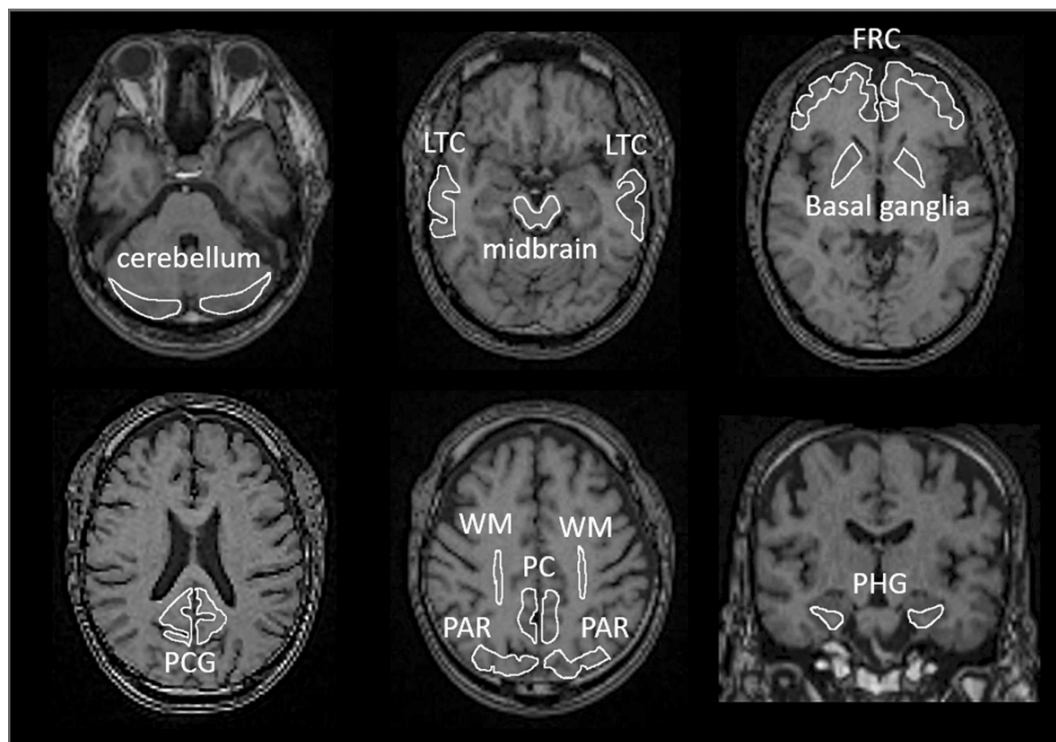


**Figure 1:** Region of interest (ROI). Each ROI was manually delineated on standard MR images to which individual PET data was standardized after acquisition of individual MR images.

LTC: Lateral Temporal Cortex; FRC: Frontal Cortex; PCG: Posterior Cingulate Gyrus; WM: White Matter; PC: Precuneus; PAR: Parietal Cortex; PHG: Parahippocampal Gyrus

eliminated. The masked images of the brain were transformed to match standard brain.

Additionally, A $\beta$  accumulation was visually evaluated based on the Japanese Alzheimer's Disease Neuroimaging Initiative (J-ADNI) Visual Criteria for PiB PET (J-ADNI\_PETQC\_Ver1.1) modified from ADNI PET core criteria [13]. Four regions selected for the assessment were the precuneus-posterior cingulate gyrus, frontal lobe, lateral temporal lobe, and lateral parietal lobe. When the accumulation in one of the above four cerebral cortices was higher than that in the white matter just below the cortex, the case was determined as positive. When none of the four cortices had higher accumulation than the white matter, the case was confirmed as negative.

### Statistical Analysis

In each ROI, age-dependency of SUVR was evaluated by calculating the Pearson's correlation coefficient ( $r$ ). Linear regression was applied to evaluate the degree of age-dependency.  $P < 0.05$  was regarded as statistically significant. To compare SUVR in MCI and AD cases with those of HC, two lines, indicating a 95% range of distribution were set in parallel to the linear regression. Group comparison of SUVR of PBB3 and PiB in predetermined ROI's was made between HC and AD using the Mann-Whitney test.

### Results

#### Demographical data

Among candidates for HC, 13 cases (7 males and 6 females, mean age 72.1 years) fulfilled the inclusion/ exclusion criteria. Scores of the

Case	Age	Gender	MMSE	HDS-R	RBMT	PiB*	In Figures 3-5
<b>Healthy Controls</b>							
1	59	M	30	30	20	(-)	○
2	62	F	28	30	23	(-)	○
3	64	M	27	30	22	(-)	○
4	64	F	30	29	17	(-)	○
5	65	M	30	30	20	(-)	○
6	73	M	26	27	21	(-)	○
7	73	M	29	27	20	(-)	○
8	75	F	29	29	21	(-)	○
9	75	F	26	29	21	(+)	●
10	81	F	29	28	20	(-)	○
11	81	M	28	25	21	(-)	○
12	82	M	30	30	19	(-)	○
13	83	F	29	30	18	(-)	○
<b>Mild Cognitive Impairment</b>							
14	81	F	30	30	nd	(-)	△
15	82	F	30	30	24	(-)	△
16	82	M	30	30	nd	(+)	▲
<b>Alzheimer's Disease</b>							
17	51	M	18	19	nd	(+)	■
18	60	F	22	27	nd	(+)	■
19	65	M	8	6	43	(+)	■
20	82	M	20	19	nd	(+)	■

MMSE: Mini-Mental State Examination; HDS-R: Revised Hasegawa Dementia Scale; RBMT: Rivermead Behavioral Memory Test; nd: not determined

PiB\*: Based on the ADNI criteria [13]

**Table 1:** Demographic data on healthy controls, cases with mild cognitive impairment and with Alzheimer's disease.

cognitive tests are shown in Table 1. PiB images were visually assessed by two raters (H.S. and J.T.), who were not informed of the clinical background, based on the J-ADNI visual criteria. Only one case (case 9) was judged as positive for A $\beta$  accumulation, and the rest were all confirmed as negative. Case 9 was excluded from further analysis of age-dependency in PBB3 and PiB accumulation in HC as the patient was believed to be in transition from HC to AD.

Three MCI cases (all in their 80's, 1 male and 2 females) were also recruited. They all obtained full marks in the MMSE and HDS-R tests, even though CDR score was 0.5 in all cases. PiB images were visually judged as positive in 1 case (case16) and as negative in 2 other cases. The PiB-positive MCI case was compared with negative cases in the following analysis.

Four patients with AD (from 51 to 82 years old, 3 males and 1 female) were also recruited. MMSE ranged from 8 to 22 points. PiB-PET images were visually all positive in these cases.

#### PBB3-PET images

Representative images of PBB3-PET images are shown in Figure 2. SUVR of PBB3 increases mildly with age in HC's (cases 1, 6 and 10), whereas the SUVR level is higher in MCI cases (case 15) and highest in AD cases (case 18). PBB3 accumulation is prominent in most cortices, excluding the primary motor and sensory cortex, the occipital lobe and the cerebellum. The basal ganglia had strong accumulation even in aged HC. Accumulation of PBB3 was also prominent in the parahippocampal gyrus on the coronal sections.

#### Age dependency in PBB3 accumulation

Distribution of PBB3-SUVR plotted against age is shown in Figure 3. Age-dependent increase in SUVR was found in all predetermined regions characteristic of AD, especially the parahippocampal gyrus ( $p=0.002$ ), frontal cortex ( $p=0.014$ ), lateral temporal cortex ( $p=0.016$ ) and posterior cingulate gyrus ( $p=0.037$ ), where the age-dependency was statistically significant. A linear regression curve and 2 parallel lines showing a range of 95% was calculated in HC (circle), excluding case 9 (filled circle), which was positive for A $\beta$ . Compared to the AD signature areas, white matter showed less steep age-dependency, whereas the slope was steeper in basal ganglia.

Among 3 MCI cases (triangle), one A $\beta$ -positive case (filled triangle) showed higher SUVR of PBB3 than the 95% range of HC, but two A $\beta$ -negative cases (open triangle) had SUVRs within the 95% range.

SUVR of PBB3 in AD cases (filled square) was all higher than the normal range in the AD signature areas. Group comparison between HC and AD without correction for their age revealed significant increases in SUVR in AD in all ROIs characteristic of AD, including the parahippocampal gyrus (Supplementary Figure 1).

#### No age dependency in PiB accumulation

In contrast to PBB3-PET images, no age-dependency in SUVR was found in any of the AD-specific areas, except the lateral temporal cortex ( $p=0.02$ ), where SUVR increased very mildly with age (Figure 4). As in PBB3 SUVR, a linear regression curve and 2 parallel lines showing the range of 95% was calculated in PiB SUVR in HC (open circle). As expected, case 9 (filled circle), which was visibly PiB-positive, had a higher PiB SUVR.

SUVR in MCI cases (triangle) was higher than that in HC, especially in case 16 (filled triangle), which was categorized as PiB-positive based on visual criteria.

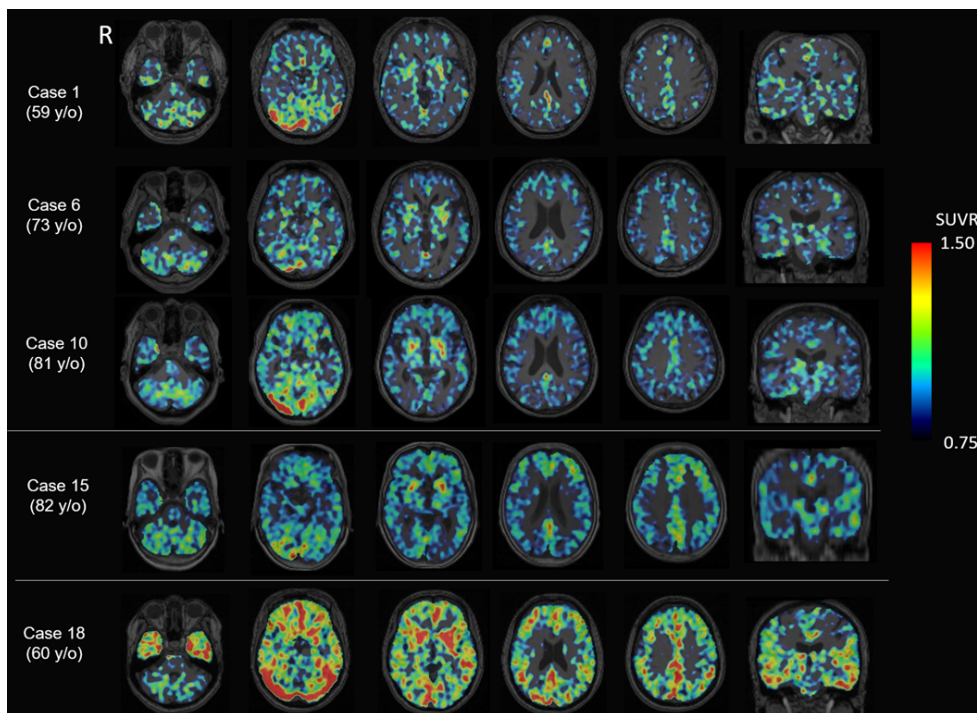


**Figure 2:** Accumulation of PBB3. SUVR of PBB3 increases mildly with age in healthy controls (cases 1, 6 and 10), whereas the level was higher in cases with mild cognitive impairment (case 15) and highest in cases with Alzheimer's disease (case 18). Accumulation of the tracer outside the brain was eliminated by masking.

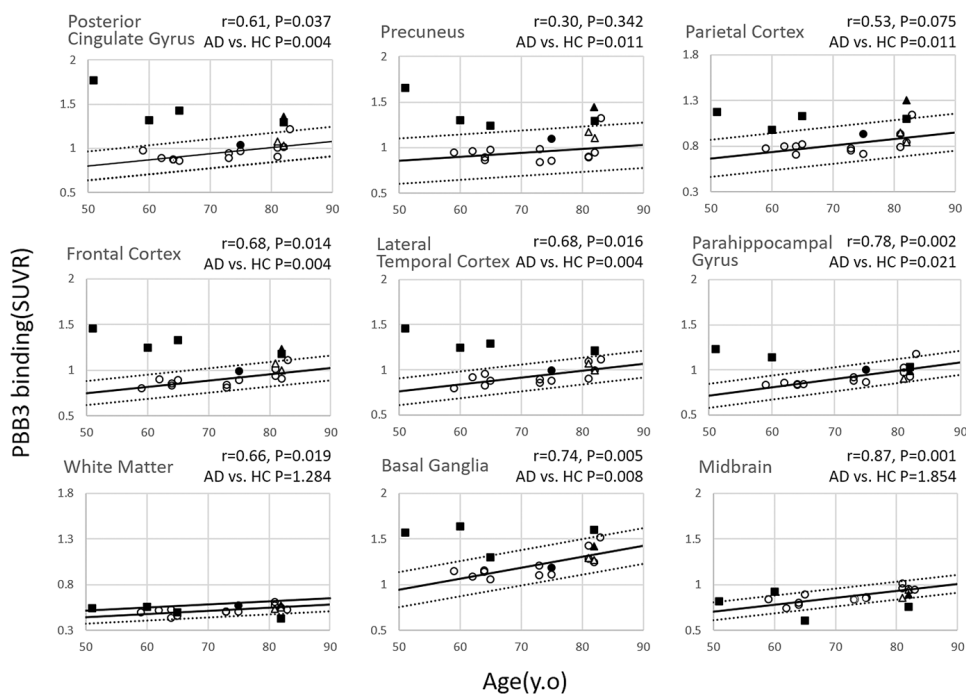


**Figure 3:** PBB3 accumulation and age. r: Correlation Coefficient. Significant correlation between age and PBB3 accumulation was found in 4 signature areas of Alzheimer's disease (AD), with the parahippocampal gyrus showing the strongest correlation. A linear regression curve and 2 parallel lines showing the range of 95% was calculated in healthy controls (HC) (open circle), excluding case 9 (filled circle), which was positive for A $\beta$ . Among 3 cases with mild cognitive impairment (triangle), one case (filled triangle) showed higher SUVR than the 95% range of HC, but the other two (open triangle) had SUVRs within the control range. SUVR of AD cases (filled square) were all higher than the normal range in most AD signature areas

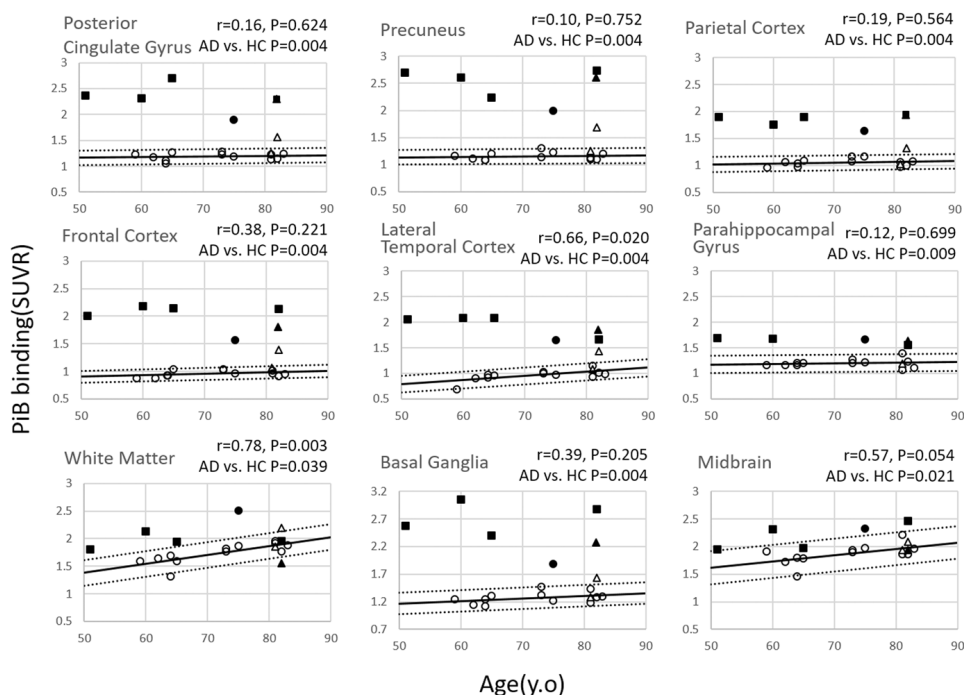


**Figure 4:** PiB accumulation and age.

r: Correlation Coefficient. No AD-specific region showed significant correlation, except the lateral temporal cortex, where SUVR increased only mildly with age. A linear regression curve and 2 parallel lines showing the range of 95% was calculated in healthy controls (open circle), excluding case 9 (filled circle). SUVR in cases with mild cognitive impairment (triangle) was higher than that in healthy controls, whereas PiB accumulation in Alzheimer's disease (AD) cases (filled square) was highest in AD signature areas as well as basal ganglia

PiB accumulation in AD cases (filled square) was highest among the 3 groups in AD signature areas as well as in basal ganglia and white matter. Group comparison between HC and AD revealed a significant increase in SUVR in AD in all ROIs characteristic of AD. Compared to the other ROIs, the parahippocampal gyrus showed very limited increase in PiB-SUVR in AD.

### Comparison of PBB3 accumulation to PiB

In HC, PBB3 SUVR increased with age, whereas PiB SUVR did not, delineating flat distribution in PBB3 vs. PiB plots (Figure 5). Among MCI cases, the tau level was mildly high, and A $\beta$  was clearly high in 1 case (case 9, filled triangle), whereas these are within higher range of HC in the other two cases (open triangle). These plots are located between higher plots in HC and those in AD. Finally, both PiB and PBB3 accumulation was significantly high in AD cases, except in the parahippocampal gyrus, where tau accumulation, but not A $\beta$  was distinctively high.

A similar pattern was found in the basal ganglia, whereas no correlation was found in the white matter and midbrain.

### Discussion

The present study showed age-dependent accumulation of tau, but not A $\beta$  in AD-related regions in HCs for the first time. In contrast, accumulation of A $\beta$  together with further accumulation of tau was observed in these regions in MCI and AD. These relationships may reflect different pathophysiological roles of tau and A $\beta$  in aging and AD pathogenesis. Namely, low doses of tau is associated with aging, and further accumulation of tau with low doses of A $\beta$  synergistically triggers

AD pathogenesis, inducing robust accumulation of both proteins as well as neurodegeneration in these regions (Supplementary Figure 2). This is still a preliminary hypothesis based on the present single report and further data acquisition is warranted to test this perspective.

Epidemiologically, the age-dependent increase in AD frequency has been well confirmed. Considering the age-dependent tau accumulation found in HC in the present study, tau may have a primary triggering effect. When gradually accumulated tau exceeds a certain threshold, pathological A $\beta$  accumulation may start inducing rapid AD progress (tau first, amyloid second theory) [4,5,14].

Interestingly, Shimada previously reported tau accumulation in AD tends to be lower in aged patients [8]. The present study also confirmed the same tendency, though the case number is too few to perform statistical analysis and to speculate any mechanisms.

Among 13 HC cases, case 9 was the only PiB-positive case based on the visual criteria. PBB3 SUVR of this case was within the higher range of HC whereas PiB SUVR was well above the 95% normal range. Apparently, tau is not the only trigger to initiate A $\beta$  accumulation. In contrast, 1 of 3 MCI cases (case 16) was PiB-positive and had a high PBB3 SUVR, far beyond the 95% normal range. This case may be in the transitional state from HC to AD. The other two MCI cases also had relatively high PBB3 SUVR.

Among AD characteristic regions, the parahippocampal gyrus showed lowest accumulation of A $\beta$  whereas tau accumulation was significant (Figure 5 and Supplementary Figure 1). In the rest of the AD-specific regions, accumulation of tau was accompanied by A $\beta$  accumulation. This regional discrepancy is in agreement with

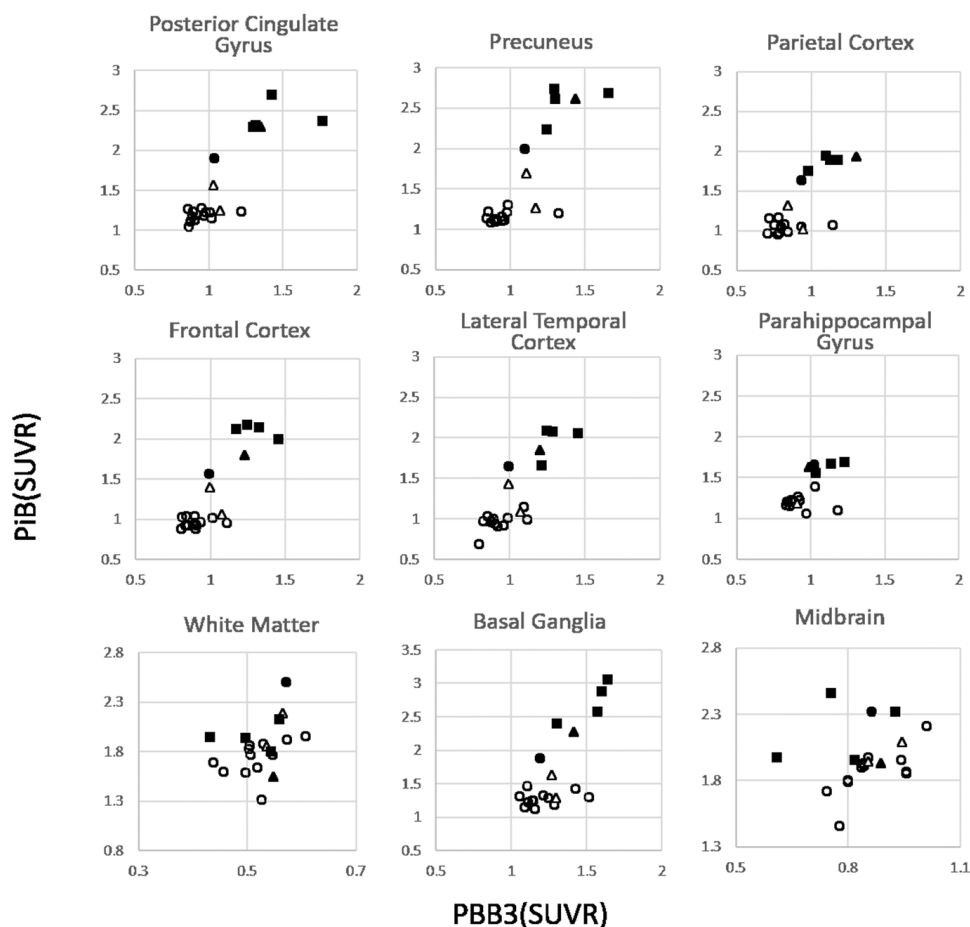


**Figure 5:** PiB vs. PBB3. In healthy controls, PBB3, but not PiB, accumulates with age. In cases with mild cognitive impairment, accumulation of PiB is more prominent than that of PBB3. In contrast, both PiB and PBB3 accumulation are significant in cases with Alzheimer's disease. Open circle: PiB-negative HC, filled circle: PiB-positive HC, open triangle: PiB-negative MCI, filled triangle: PiB-positive MCI filled square: PiB-positive AD.

pathological findings [2]. Based on Braak staging [2], our cases in younger controls may be in stage I and older controls in stage II. MCI cases may be in stages III and IV. AD cases represent stages V and VI.

Age-dependent tau accumulation was also found in the white matter and midbrain in HCs, whereas further accumulation of tau in MCI and AD cases was not observed in these regions. Considering common pathological findings that AD pathology is not outstanding in these regions, age-dependent tau accumulation in these regions may not be involved in the pathogenesis of AD.

Accumulation of PBB3 in basal ganglia is currently controversial as basal ganglia express small amounts of paired helical filament [2]. Ng et al., recently reported off-target binding of 18F-THK5351, another tau tracer, to monoamine oxidase-B (MAO-B), which is highly expressed in basal ganglia [15]. Unlike 18F-THK5351, 18F-THK5117 and 18F-THK5317, PBB3 is not a quinoline derivative and may not be influenced by MAO-B. Significantly higher PBB3 SUVRs in AD than in HC clearly indicate the pathological relevance of PBB3 accumulation in the basal ganglia.

Utilizing 18F-AV1451, Scholl et al. reported similar tau depositions in the aging brains of HCs [16]. Accumulation was higher in PiB-positive HCs and much higher in AD. Unlike our control group, with ages ranging from the 50's to the 80's, their young controls were 22.2

years old on average, and old controls were 78.6 years old on average. Additionally, half of the older controls were PiB-positive, whereas our control group excluded a PiB-positive case for the analysis of aging and proved detailed age-dependency. We previously showed that the rate of PiB positivity increases with age in HCs [17]. In the present study, we demonstrated that PiB-positive cases have high PBB3 SUVR. Therefore, analysis of aging brains with the inclusion of a PiB-positive case in the HCs can confoundedly yield age-dependency in PBB3 SUVR. We excluded that possibility in the present study.

Neuropathologically, age-related tau accumulation without A $\beta$  in the medial temporal lobe, basal forebrain, and brainstem is postulated to represent primary age-related tauopathy (PART) [3,6]. The concept of PART covers cases with normal cognitive function to those with profound cognitive impairment. The HC group in the present study showed age-dependent tau accumulation in the AD-related cortices, which may relate to the PART pathology, although the distribution of tau was more diffuse in the present study. In contrast, MCI cases and AD cases demonstrated higher and highest tau deposition together with A $\beta$ . Based on this gradual tau accumulation from HC to AD, we postulate that age-dependent tau accumulation in HC represents a high risk for developing AD rather than just A $\beta$ -independent pathophysiology [6].

There are several limitations of the study. First, data on the specificity

of the PBB3 tracer is still limited [16]. PBB3 may have off-target bindings, such as MAO-B, for 18F-THK5351, 18F-THK5117 and 18F-THK5317. Second, the present study is a cross-sectional study. Gradual accumulation of tau and A $\beta$  observed through transition from MCI to AD should be confirmed serially. Similarly, high accumulation of tau in aging HCs should be tested as a risk for later AD development by a longitudinal study.

## Conclusion

We report that mild accumulation of tau without A $\beta$  was found in AD-specific areas in aging brains. Higher accumulation of tau was associated with A $\beta$  accumulation in MCI and AD patients and may be involved in triggering the neurodegenerative process.

## Acknowledgement

The authors thank Ms. M Ando and Ms. N Kotani (Osaka City University) for psychological tests.

## Funding

The present study was financially supported by the NIRS/QST grant (Japan Agency for Medical Research and Development #16768966), in which Osaka City University was involved as a collaborating facility.

## References

- Williams DR (2006) Tauopathies: Classification and clinical update on neurodegenerative diseases associated with microtubule-associated protein tau. *Intern Med J* 36: 652-660.
- Braak H, Braak E (1991) Neuropathological staging of Alzheimer-related changes. *Acta Neuropathol* 82: 239-259.
- Crary JF, Trojanowski JQ, Schneider JA, Abisambra JF, Abner EL, et al. (2014) Primary age-related tauopathy (PART): A common pathology associated with human aging. *Acta Neuropathol* 128: 755-766.
- Arriagada PV, Growdon JH, Hedley-Whyte ET, Hyman BT (1992) Neurofibrillary tangles but not senile plaques parallel duration and severity of Alzheimer's disease. *Neurology* 42: 631-639.
- Nelson PT, Alafuzoff I, Bigio EH, Bouras C, Braak H, et al. (2012) Correlation of Alzheimer disease neuropathologic changes with cognitive status: A review of the literature. *J Neuropathol Exp Neurol* 71: 362-381.
- Crary JF (2016) Primary age-related tauopathy and the amyloid cascade hypothesis: The exception that proves the rule? *J Neurol Neurosurg* 1: 53-57.
- Maruyama M, Shimada H, Suhara T, Shinotoh H, Ji B, et al. (2013) Imaging of tau pathology in a tauopathy mouse model and in Alzheimer patients compared to normal controls. *Neuron* 79: 1094-108.
- Shimada H, Kitamura S, Shinotoh H, Endo H, Niwa F, et al. (2017) Association between Abeta and tau accumulations and their influence on clinical features in aging and Alzheimer's disease spectrum brains: A [11C]PBB3-PET study. *Alzheimers Dement (Amst)* 6: 11-20.
- Albert MS, DeKosky ST, Dickson D, Dubois B, Feldman HH, et al. (2011) The diagnosis of mild cognitive impairment due to Alzheimer's disease: Recommendations from the national institute on aging-Alzheimer's association workgroups on diagnostic guidelines for Alzheimer's disease. *Alzheimers Dement* 7: 270-279.
- Dubois B, Feldman HH, Jacova C, Hampel H, Molinuevo JL, et al. (2014) Advancing research diagnostic criteria for Alzheimer's disease: The IWG-2 criteria. *Lancet Neurol* 13: 614-629.
- Hashimoto H, Kawamura K, Igarashi N, Takei M, Fujishiro T, et al. (2014) Radiosynthesis, photoisomerization, biodistribution and metabolite analysis of 11C-PBB3 as a clinically useful PET probe for imaging of tau pathology. *J Nucl Med* 55: 1532-1538.
- Kimura Y, Ichise M, Ito H, Shimada H, Ikoma Y, et al. (2015) PET quantification of tau pathology in human brain with 11C-PBB3. *J Nucl Med* 56: 1359-1365.
- Jagust WJ, Bandy D, Chen K, Foster NL, Landau SM, et al. (2010) The ADNI PET core. *Alzheimers Dement* 6: 221-229.
- van Rossum IA, Vos SJ, Burns L, Knol DL, Scheltens P, et al. (2012) Injury markers predict time to dementia in subjects with MCI and amyloid pathology. *Neurology* 79: 1809-1816.
- Ng KP, Pascoal TA, Mathotaarachchi S, Therriault J, Kang MS, et al. (2017) Monoamine oxidase B inhibitor, selegiline, reduces 18F-THK5351 uptake in the human brain. *Alzheimers Res Ther* 9: 25.
- Scholl M, Lockhart SN, Schonhaut DR, O'Neil JP, Janabi M, et al. (2016) PET imaging of tau deposition in the aging human brain. *Neuron* 89: 971-982.
- Mino T, Saito H, Takeuchi J, Ito K, Takeda A, et al. (2017) Cerebral blood flow abnormality in clinically diagnosed Alzheimer's disease patients with or without amyloid  $\beta$  accumulation on positron emission tomography. *Neurol Clin Neurosci* 5: 55-59.